ISOTROPIC ETCHING OF 111 SCS FOR WAFER-SCALE MANUFACTURING OF PERFECTLY HEMISPHERICAL SILICON MOLDS

Laura C. Fegely, David N. Hutchison, and Sunil A. Bhave
OxideMEMS Lab, Cornell University, Ithaca, NY, USA

ABSTRACT

This paper reports the results of a side-by-side comparison study of HF-HNO_3 isotropic etching of circular pits in <111> and <100> single crystal silicon (SCS). These etched holes will be used as sacrificial molds for micro-scale hemispherical resonator gyroscopes (HRGs) made using hemispherical shell resonators. Geometric uniformity of the mold is critical for HRG applications in order to achieve degenerate resonant modes and high optical and mechanical quality factors (Q). <111> wafers were found to provide excellent isotropic etching in the surface plane under all tested etching conditions with an average of only ~1.4% radial variation, as compared to ~3.2% variation for <100> wafers. The molds tested had an average radius of 41 μm, and depth of 35 μm, with a maximum of radius 92 μm with a depth of 95 μm.

KEYWORDS

Isotropic wet etching, hemispherical shell, gyroscope, 3D micromachining

I. INTRODUCTION

Traditional HRG's are navigational grade gyroscopes used in inertial navigation units and satellite platform positioning. However, they are expensive, bulky, and laborious to fabricate. As HRGs are scaled down to the micro-scale to enable wafer-scale manufacturability, it becomes difficult to achieve high quality factors, degenerate oscillation frequencies and the negation of parasitic vibration modes [1]. Achieving this behavior requires very good uniformity of the radius, particularly in the x-y plane (as shown in Fig. 1), and very low surface roughness. HRGs that also have constant radius along the z-axis have lower anchor losses, providing the high energy dissipation time constant necessary for whole angle operation. One method of fabricating these micro-scale HRGs is to use an isotropic etch to first create a hemispherical bowl, and then conformally deposit the resonator material. After the rim of the bowl is defined using standard lithography and etching techniques, an isotropic etch can again be used to release the structures and create the stems. This method of fabrication requires the initial isotropic etch to be very isotropic and smooth. Figures of merit used to characterize the uniformity of the etch both in-plane and in the z-direction are defined in Eq. 1-3, where R_{avg} is an average of measured R values as shown in Figure 1.

$$\%_{PE} = \left(\frac{R'}{R_{avg}} - 1 \right) \times 100 \qquad (1)$$

$$\sigma_{rad}^2 = \frac{1}{n-1} \sum_{i=1}^{n} \left(R_{avg} - R_i \right)^2 \qquad (2)$$

$$\varepsilon_z = \left| \frac{d}{R_{avg}} - 1 \right| \qquad (3)$$

Thus, looking at the resultant hemispheres in Fig. 1, the optimal geometry would be type I. Preferential etching in the x-y plane as in type II will lead to a loss of degeneracy, which is unacceptable. Non-uniformity in the z direction, as in type III, may be acceptable but reduces the Q of the device.

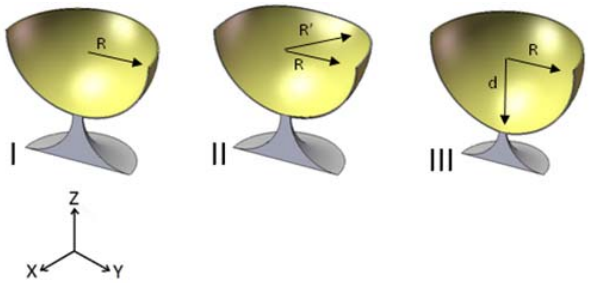

Figure 1: Shell resonators resulting from thin film deposition onto molds, and release of the structures. Shell geometries correspond to a perfectly isotropic etch (I), an etch with preferential etching only in the X-Y plane (II), and an etch showing X-Y, but not Z isotropic etching (III). R' is the axis which is preferentially etched in the X-Y plane, while actual depth measurements are denoted by d.

Two of the most common isotropic silicon etches are XeF_2 and HF-Nitric acid etching. XeF_2 is a gas phase etch, in which the XeF_2 sublimates at room temperature to etch silicon according to the equation:

$$2XeF_2 + Si \rightarrow 2Xe + SiF_4 \qquad (4)$$

Surface roughness and higher lateral etch rates can often be a problem with this etch for the purposes of creating molds for hemispherical shell resonators, though these effects can be decreased by lowering the etch pressure or adding N_2 as a buffer gas. HNA, which is typically a combination of HF and Nitric acid diluted by Acetic acid or water, makes use of the oxidizing properties of Nitric acid in combination with the SiO_2 consuming properties of HF to isotropically etch silicon. The etch reactions for the HNA etch are:

$$\left.\begin{array}{l} 3Si + 4HNO_3 \rightarrow 3SiO_2 + 4NO + 2H_2O \\ 3SiO_2 + 18HF \rightarrow 3H_2SiF_6 + 6H_2O \end{array}\right\} \qquad (5)$$

The diluent used can be either water or acetic acid. Acetic acid has the benefit of having a lower dielectric constant than water, causing less dissociation of the nitric acid and giving more oxidation power to the etch, but due to waste disposal restrictions, water is sometimes preferred. Throughout the reaction, sites on the silicon randomly become oxidation or reduction sites, with each point becoming both an anode and a cathode site over time. If the time spent in each of these states is the same, the etch will be isotropic, but if not than preferential etching will occur [5].

II. EXPERIMENTAL SETUP

The etching experiment was performed in three stages. In the first stage, a basic comparison of XeF_2 and HNA etching was performed, showing that HNA wet etching was preferential to XeF_2 etching for its reduced surface roughness and constant out-of-plane radius, as shown in Figure 2 below.

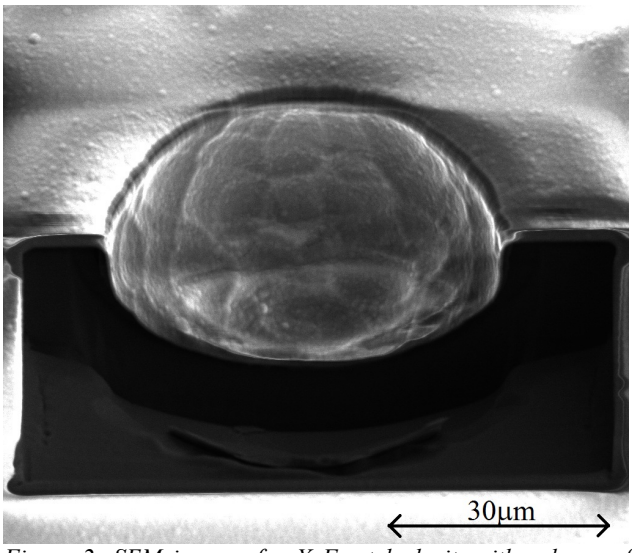

Figure 2: SEM image of a XeF_2 etched pit, with a layer of silicon nitride deposited on top, and a cross section removed using a focused ion beam to view the cross section of the etch. Pitting and shallowing of the etch is clearly seen.

Additionally, the required size of the etch windows in the mask were determined to be greater than 10µm, because windows smaller than this were seen to cause significant diffusion limiting of the etch. However, it was also seen that the HF-HNO_3 etch on <100> silicon wafers preferentially etches the [110] plane over the [100] plane [2]. Previous solutions to this problem [2][3] involved controlling both the chemical ratio and the temperature to find an etch that did not show this preferential etching behavior. These solutions, however, create a tradeoff between etch rate controllability and the anisotropy [2]. For the extremely stringent critical dimensions required for micro-scale gyroscopes, this tradeoff has no solution which is acceptable for both geometry and manufacturability, so a new approach was needed.

Thus in the second stage of the experiment, an attempt to optimize the HNA etch was performed. Agitation rate, chemical ratio, and etch window size were all known to be critical features in a wet isotropic etch using HF and Nitric acid. However, there was almost nothing in the way of detailed studies of HNA etching of <111> SCS. Believing that the more dense surface of the <111> wafers may reduce the effects of preferentially etched planes, we hypothesized that it may etch more isotropically.

Using 180 nm of Si_3N_4 as the mask, <100> and <111> wafers were patterned with circular etch windows and diced to create homogenous samples. The design variables tested in addition to wafer orientation were:

- Mask etch window diameter – 20µm, 30µm, 40µm, 50µm
- Chemical ratio – sample space as shown in Fig. 3
- Agitation rate – no agitation, agitation by hand, agitation in ultrasonic bath

A total of 60 samples were etched for a period of 120s per sample. After removal of the nitride mask, the depth of etch and in-plane radial uniformity were determined using a Wyko optical profilometer as shown in Fig. 4, and full etch profiles were revealed using a focused ion beam and SEM (Fig. 5).

In the final stage of the experiment, the thickness of the nitride mask was increased, and in place of the agitation rate variable, temperature was tested. The same variables were used for the etch window diameter and wafer orientations. Additionally, all the chemical ratios (alphabetically labeled in Figure 3) were characterized except sample points H and I, which had shown no significant etching in the second stage of the experiment.

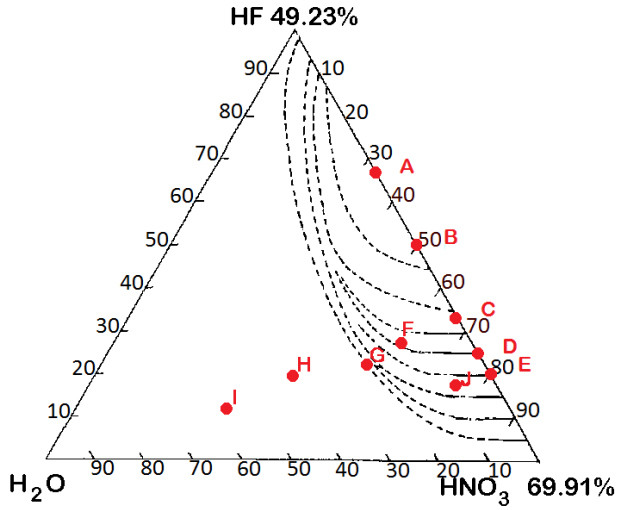

Figure 3: The iso-etch curves for HF-Nitric-H_2O etching of silicon taken from [6], with red dots representing sampled chemical ratios. The innermost curve (inside which lie points A and B) represents the highest etch rates.

III. RESULTS

The effects of etch mask window size, agitation rate, and etchant composition were seen to follow many of the same trends in <111> silicon as seen in <100> oriented wafers. The difference between the two lies in the fact that

the inherent anisotropy in the <111> wafers seems to be much smaller, allowing for lower temperature, and thus more rate-stable etches to be performed. Looking at the more anisotropic etches that were performed, preferential etch directions can be seen. For the <100> wafers, a square shape with a maximum etch radius at 45° between the x and y axes was seen. The <111> wafers showed a hexagonal shape with a maximum etch radius along the x axis. These maximum radii are those denoted by R' in Figures 4a and 4b.

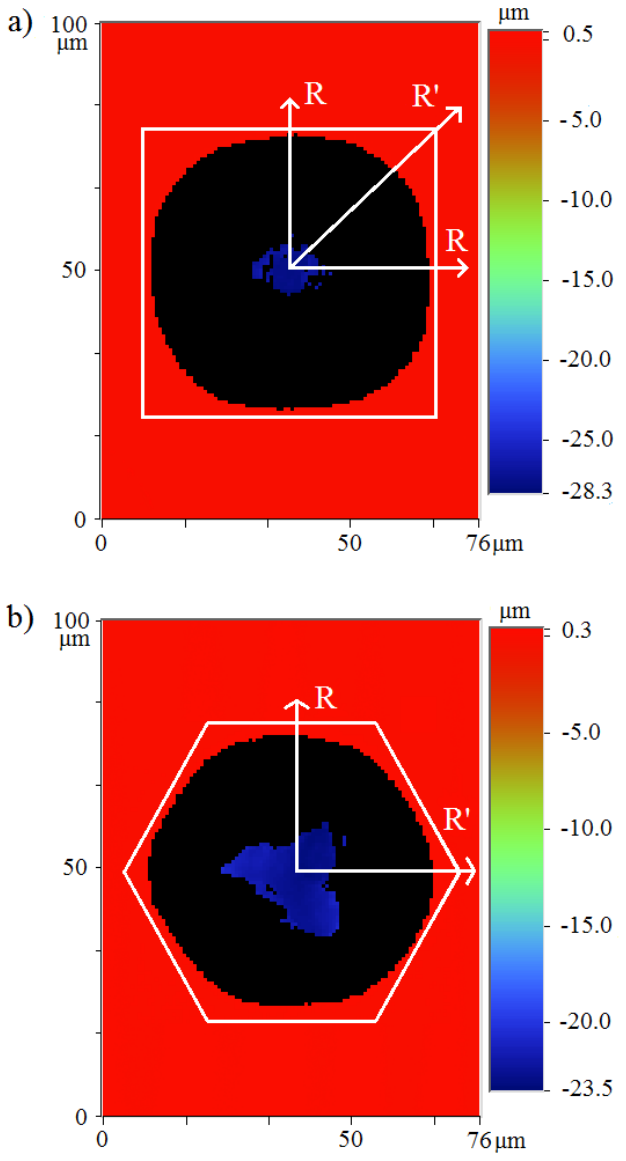

Figure 4: Results from the optical profilometer for etchant group F, 20 µm diameter etch window samples agitated by hand. Etchant group F was the least isotropically etched and is shown here to emphasize the method of measuring R and R'. The lateral etch rates and depths appear to be similar, though preferential etching can be seen in the square shape of the <100> sample and the slight hexagonal shape of the <111> sample. These shapes tend to become more defined as the ratio of Nitric:HF Acid increases, as well as by increasing the proportion of H_2O.

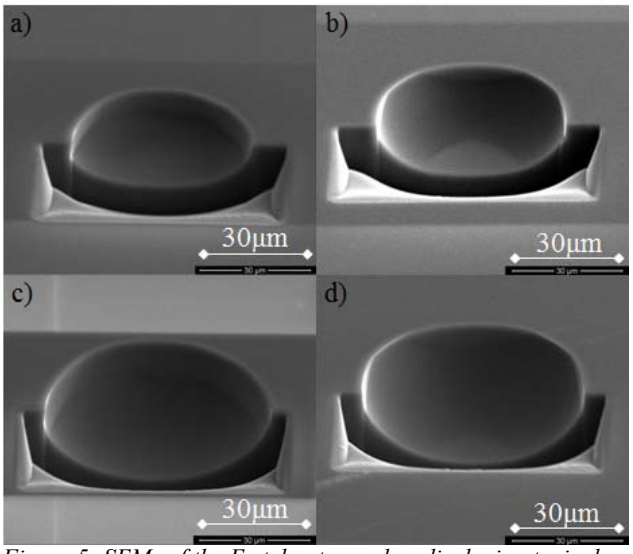

Figure 5: SEMs of the E etchant samples, displaying typical agitation dependent profiles. The samples are angled at 52 ^{0}, with the <111> wafers displayed on the left column and the <100> wafers on the right. (a) and (b) correspond to samples etched without agitation and (c) and (d) to samples etched in an ultrasonic bath. The samples with no agitation show a clear shallowing of the etch.

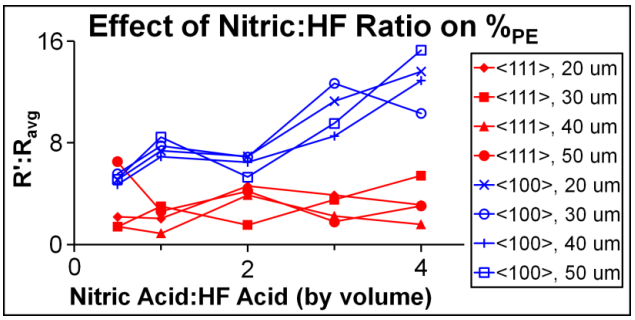

Figure 6: The effect of chemical ratio of etchant on preferential etching for samples without agitation (Etchants A through E, for each of the etch window sizes). Note that except for one outlier, all <111> samples show greater uniformity than <100>. Additionally, we see further confirmation that higher Nitric acid:HF ratios lead to more preferential etching.

Etch window diameter: Even after subtraction of the etch window diameter from the measured diameters of each of the etched molds, the etch rates for molds etched with larger etch windows were seen to be consistently higher. This would seem to imply that diffusion is still a limiting factor in the etch rate, but this may not actually be the case. Because part of the nitric acid reaction is an autocatalytic reaction in which HNO_2, a reaction byproduct, is regenerated by the reaction itself, the HNA etch rate can actually increase as silicon is consumed. Thus the higher etch rates seen for larger etch windows may also be due to this feedback loop in the HNA etch reaction.

Chemical Ratio: Several notable trends were seen with changes in the chemical ratio of the etches. Sample points A and B as shown in Figure 3 showed the highest etch rates, with etch rate decreasing with addition of nitric acid. Similar results are seen with the addition of water. These trends are to be expected from the etch rate curves shown in the etch triangle in Figure 3, but the more interesting effect is that preferential etching seems to follow these same trends. This seems to suggest that preferential etching and the speed of the etch could be related. Some examples of the increase in preferential etching with increase in proportion of nitric acid are shown in Figure 6.

Agitation Rate: As would be expected, the samples without agitation etched more shallowly, with hand and ultrasonic agitation giving similarly deeper etches which were more isotropic in the z-axis. No significant trend between agitation rate and x-y plane anisotropy was seen, but since an increased etch rate was seen without a decrease in preferential etching, a direct correlation between the etch rate and the amount of preferential etching can be discarded. A loss in yield was seen with the hand and ultrasonically agitated samples, particularly in the high HF chemical ratios due to breakage caused to the nitride etch mask. In the third stage of testing, a thicker nitride mask eliminated this problem.

Temperature: Increases in temperature showed a clear correlation to increases in etch rate, particularly in etches which were high in HF. As shown in Figure 7, the rate at which the etch rate increases is highest for Etchant B, and decreases with increasing nitric acid ratios.

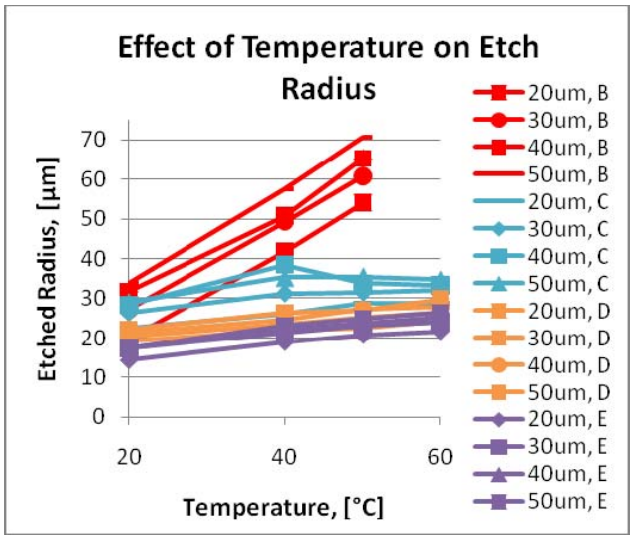

Figure 7: Chart showing the effects of temperature on the etched radius for <111> samples for Etchants B - E. The etch radius is determined by subtracting out the etch window dimensions, so these values are effectively normalized.

Wafer Orientation: With regards to etch rate both in the x-y plane and along the z-axis, no significant difference was seen between the <100> and <111> oriented wafers. However, the <111> wafers showed less preferential etching across the board, with an average $\%_{PE}$ of 1.4%, less than half of the average <100> $\%_{PE}$ of 3.2%. This reduction in preferential etching could be in part due to the higher order shape in seen in the <111> preferential etching, leading to a better initial approximation to a circular shape.

IV. CONCLUSIONS

Through this work, an isotropic etch for the purpose of creating very isotropic molds for the fabrication of micro-scale hemispherical resonator gyroscopes was optimized. Particularly, high HF content and <111> silicon wafer orientation showed a reduction in preferential etching in the x-y plane, while z-axis uniformity is optimized using agitation. Avoiding the higher, less controllable etch rates of high temperature HNA etches, our experiments show that <111> wafers are superior to <100> wafers for manufacturing 3-D isotropic MEMS devices.

ACKNOWLEDGEMENTS

We would like to recognize the use of the Cornell Nanofabrication Facility and the Cornell Center for Materials Research through which this work was performed.

REFERENCES

[1] E.J. Eklund, A.M. Shkel, "Glass Blowing on a Wafer Level", *JMEMS*, Vol. 16 Issue 2 (April 2007), pp. 232-239.

[2] H. Hashimoto, *et al*, "Chemical Isotropic Etching of Single-Crystal Silicon for Acoustic Lens of Scanning Acoustic Microscope", *JJAP*, 32 (1993), pp. 2543-2546.

[3] S. Wise, *et al*, "A Method for the Mass Production of ICF Targets", *Journal of Nuclear Materials*, 85&86, pp. 103-106.

[4] M.J. Madou, "Fundamentals of Microfabrication: The Science of Miniturization", 2nd ed., CRC Press, New York, NY, pp. 208-212.

[5] D.R. Turner, "On the Mechanism of Chemically Etching Germanium and Silicon." *Journal of The Electrochemical Society* 107.10 (1960): 810. Print.

[6] H. Robbins, and B. Schwartz. "Chemical Etching of Silicon." *Journal of The Electrochemical Society* 107.2 (1960): 108-11. Print.

CONTACT

* L.C. Fegely, tel: 1-717-725-2478; lcf36@cornell.edu